RESEARCH ARTICLE

Precision Targeted Therapy with BLU-667 for *RET*-Driven Cancers

Vivek Subbiah[1], Justin F. Gainor[2], Rami Rahal[3], Jason D. Brubaker[3], Joseph L. Kim[3], Michelle Maynard[3], Wei Hu[3], Qiongfang Cao[3], Michael P. Sheets[3], Douglas Wilson[3], Kevin J. Wilson[3], Lucian DiPietro[3], Paul Fleming[3], Michael Palmer[3], Mimi I. Hu[4], Lori Wirth[2], Marcia S. Brose[5], Sai-Hong Ignatius Ou[6], Matthew Taylor[7], Elena Garralda[8], Stephen Miller[3], Beni Wolf[3], Christoph Lengauer[3], Timothy Guzi[3], and Erica K. Evans[3]

ABSTRACT The receptor tyrosine kinase rearranged during transfection (RET) is an oncogenic driver activated in multiple cancers, including non–small cell lung cancer (NSCLC), medullary thyroid cancer (MTC), and papillary thyroid cancer. No approved therapies have been designed to target RET; treatment has been limited to multikinase inhibitors (MKI), which can have significant off-target toxicities and limited efficacy. BLU-667 is a highly potent and selective RET inhibitor designed to overcome these limitations. *In vitro*, BLU-667 demonstrated ≥10-fold increased potency over approved MKIs against oncogenic RET variants and resistance mutants. *In vivo*, BLU-667 potently inhibited growth of NSCLC and thyroid cancer xenografts driven by various *RET* mutations and fusions without inhibiting VEGFR2. In first-in-human testing, BLU-667 significantly inhibited RET signaling and induced durable clinical responses in patients with *RET*-altered NSCLC and MTC without notable off-target toxicity, providing clinical validation for selective RET targeting.

SIGNIFICANCE: Patients with *RET*-driven cancers derive limited benefit from available MKIs. BLU-667 is a potent and selective RET inhibitor that induces tumor regression in cancer models with *RET* mutations and fusions. BLU-667 attenuated RET signaling and produced durable clinical responses in patients with *RET*-altered tumors, clinically validating selective RET targeting. *Cancer Discov; 8(7); 836–49. ©2018 AACR.*

See related commentary by Iams and Lovly, p. 797.

INTRODUCTION

Targeting oncogenic driver kinases with specifically tailored inhibitors has transformed the management of a variety of hematologic malignancies and solid tumors. First-generation kinase inhibitors directed against oncogenic drivers such as *BCR–ABL* fusions (imatinib), *EGFR* mutations (erlotinib and gefitinib), and *ALK* rearrangements (crizotinib) have demonstrated vast improvements over cytotoxic chemotherapy in chronic myelogenous leukemia and kinase-driven non–small cell lung cancer (NSCLC), respectively (1–4). These early successes established a new treatment paradigm for the use of targeted kinase inhibitors to benefit genetically defined patient populations. Despite the effectiveness of these approaches, however, acquired resistance to therapy has emerged as a major clinical challenge, spurring efforts to develop more potent and selective next-generation kinase inhibitors that also encompass activity against observed and predicted resistance mutations (5–9).

Rearranged during transfection (RET) is a receptor tyrosine kinase and *bona fide* oncogene that drives various cancers (10–16). RET normally plays a critical role in kidney morphogenesis and embryonic development of the enteric nervous system. However, oncogenic *RET* alterations promote ligand-independent, constitutive RET kinase activation, which drives tumorigenesis. To date, two major mechanisms of RET kinase activation have been described: (i) *RET* point mutations and (ii) *RET* gene rearrangements. RET missense mutations can occur in extracellular cysteine residues (e.g., C620R and C634R/W), which trigger aberrant receptor dimerization, or in the intracellular kinase domain, which promotes ligand-independent kinase activation (e.g., V804L/M, M918T; ref. 17). Activating point mutations are most commonly found in medullary thyroid cancer (MTC); approximately 50% of sporadic MTCs harbor activating *RET* mutations, and nearly all cases of familial MTC contain a germline activating *RET* mutation (17, 18). Alternatively, RET activation can occur via gene rearrangement. *RET* rearrangements create a fusion protein juxtaposing the RET kinase domain and a dimerization domain of another protein, creating a constitutively activated dimer (19). RET fusions are seen in 10% to 20% of papillary thyroid cancer (PTC), 1% to 2% of NSCLCs, and multiple other cancer subtypes, including colorectal and breast cancers (10–18). Together, these data indicate that dysregulated RET signaling can act as an important driver across multiple tumor indications.

Although *RET* was one of the first kinase fusions cloned from an epithelial tumor (20), patients with *RET*-driven cancers have derived only modest benefit from RET-directed strategies to date. It should be noted, however, that RET therapies thus far have largely centered around multikinase

[1]Department of Investigational Cancer Therapeutics, Division of Cancer Medicine, The University of Texas MD Anderson Cancer Center, Houston, Texas. [2]Department of Medicine, Massachusetts General Hospital, Boston, Massachusetts. [3]Blueprint Medicines Corporation, Cambridge, Massachusetts. [4]Department of Endocrine Neoplasia and Hormonal Disorders, The University of Texas MD Anderson Cancer Center, Houston, Texas. [5]Abramson Cancer Center, University of Pennsylvania, Philadelphia, Pennsylvania. [6]Chao Family Comprehensive Cancer Center, University of California Irvine Medical Center, Irvine, California. [7]The Knight Cancer Institute, Oregon Health and Science University, Portland, Oregon. [8]Vall d'Hebron Institute of Oncology (VHIO), Barcelona, Spain.

Note: Supplementary data for this article are available at Cancer Discovery Online (http://cancerdiscovery.aacrjournals.org/).

V. Subbiah and J.F. Gainor are co–first authors and contributed equally to this article.

Corresponding Author: Erica K. Evans, Blueprint Medicines, 45 Sidney Street, Cambridge, MA 02139. Phone: 617-714-6675; E-mail: eevans@blueprintmedicines.com

doi: 10.1158/2159-8290.CD-18-0338

inhibitors (MKI) that have been repurposed to treat patients with *RET* alterations. For example, the MKIs cabozantinib and vandetanib were originally designed to target other kinases, such as VEGFR2, tyrosine–protein kinase MET, and EGFR, and they inhibit these targets more potently than RET (21, 22). Cabozantinib and vandetanib are both approved for the treatment of patients with metastatic or locally advanced MTC and have documented activity in patients with *RET* fusion–driven NSCLC, yet each agent has produced limited disease control and lower response rates compared with selective kinase inhibitors targeting other oncogenic drivers in NSCLC (23–26). In addition, the significant side-effect profiles of each can either limit use in certain patients or limit the dose that patients can tolerate. Furthermore, these agents are biochemically inactive against the RET V804L/M mutants. This gatekeeper position is associated with acquired resistance to tyrosine kinase inhibitors in other targeted therapy/kinase pairs, and mutations at this residue act as primary driver mutations in a subset of hereditary MTCs. Additional MKIs with ancillary RET activity, such as sunitinib, lenvatinib, regorafenib, and RXDX-105, have also been tested in *RET*-driven tumors with equally disappointing results (27). Together, these findings have led some investigators to question whether *RET* is a dominant oncogenic driver or whether currently available MKIs insufficiently inhibit RET *in vivo* due to narrow therapeutic indices.

Here, we describe BLU-667, a next-generation small-molecule RET inhibitor specifically designed for highly potent and selective targeting of oncogenic RET alterations, including the most prevalent RET fusions (e.g., KIF5B–RET and CCDC6–RET) and RET-activating mutations (e.g., C634W, M918T, and V804L/M). BLU-667 demonstrated increased RET potency and selectivity relative to MKIs both *in vitro* and in *in vivo* models of *RET*-driven thyroid, lung, and colorectal cancers. In early clinical testing, BLU-667 attenuated RET signaling and induced durable responses in patients with *RET*-altered NSCLC and MTC without notable off-target toxicity, establishing initial proof of principle for highly selective RET targeting in *RET*-driven malignancies.

RESULTS

BLU-667 Potently and Selectively Inhibits RET

A library of over 10,000 agnostically designed kinase inhibitors with greater than 60 chemical scaffolds and annotated versus the human kinome was interrogated to identify compounds with inhibitory activity against wild-type (WT) RET and oncogenic RET variants (M918T, V804L, and V804M), while maintaining selectivity against other human kinases. Iterative medicinal chemistry optimization was performed with these initial compounds to improve RET potency, selectivity, and pharmaceutical properties, leading to the generation of BLU-667 (Fig. 1A). In biochemical assays, BLU-667 inhibited the kinase activity of WT RET with subnanomolar potency (IC_{50} 0.4 nmol/L; Table 1). Compared with the MKIs cabozantinib, vandetanib, and RXDX-105 (IC_{50} 11, 4, and 3 nmol/L, respectively), BLU-667 was 8- to 28-fold more potent against WT RET (Fig. 1B; Table 1). Moreover, BLU-667 demonstrated potent activity (IC_{50} 0.4 nmol/L) against common oncogenic RET alterations, including RET^{M918T}, an

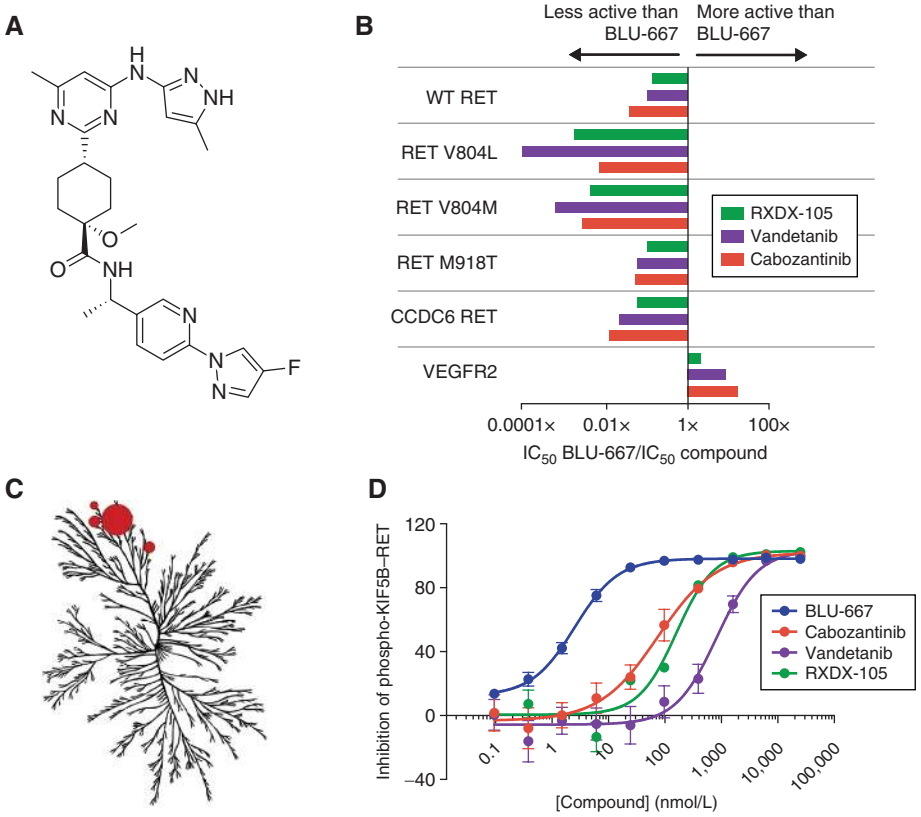

Figure 1. BLU-667 is a potent and selective inhibitor of RET. **A,** Chemical structure of BLU-667. **B,** Biochemical IC_{50} comparison of BLU-667 and cabozantinib, vandetanib, and RXDX-105 on WT RET, RET mutants, and VEGFR2 represented by the BLU-667 IC_{50} value divided by the IC_{50} of each compound. **C,** Kinome tree depicting selectivity of BLU-667. IC_{50} relative to RET is depicted by the size of the circles, where the large circle represents RET, the medium circles represent kinases less than 50 × of the RET IC_{50}, and the small circles represent kinases less than 100 × of the RET IC_{50}. Kinome illustration reproduced courtesy of Cell Signaling Technology. **D,** Concentration–response curves for BLU-667, cabozantinib, vandetanib, and RXDX-105 measuring inhibition of KIF5B–RET autophosphorylation in a cellular setting. Data are the mean ± SD. SD, standard deviation.

Table 1. Biochemical potency of BLU-667 and MKIs against activated RET mutants and fusion variants

	Biochemical IC_{50}, nmol/L					
Compound	WT RET	RET V804L	RET V804M	RET M918T	CCDC6–RET	VEGFR2
BLU-667	0.4	0.3	0.4	0.4	0.4	35
Cabozantinib	11	45	162	8	34	2
Vandetanib	4	3,597	726	7	20	4
RXDX-105	3	188	102	4	7	17

activating mutation found in MTC, as well as the CCDC6–RET fusion observed in PTC and NSCLC (17, 28).

A common therapeutic vulnerability of kinase inhibitors in the clinic is the development of on-target resistance mutations, particularly at the gatekeeper position, that sterically hinder inhibitor binding. These mutations have been observed in chronic myeloid leukemia (BCR–ABL^{T315I}), EGFR-mutant NSCLC ($EGFR^{T790M}$), and *ALK*-rearranged NSCLC (ALK^{L1196M}; ref. 6). Interestingly, RET gatekeeper mutations at the V804 residue (V804L and V804M) can occur as germline mutations in patients with MTC (29) and have also been shown to confer resistance to MKIs *in vitro* (29). Cabozantinib and vandetanib were poor inhibitors of these mutants with approximately 100- to 10,000-fold higher IC_{50}s than against WT RET (Fig. 1B; Table 1). By contrast, BLU-667 was designed to inhibit these resistance mutations and demonstrated the same subnanomolar potency as observed against WT RET (IC_{50} of 0.3 and 0.4 nmol/L for RET^{V804L} and RET^{V804M}, respectively; Fig. 1B; Table 1).

Currently available MKIs with RET activity (e.g., cabozantinib and vandetanib) are characterized by activity against multiple kinase targets, most notably the receptor tyrosine kinase VEGFR2, which regulates angiogenesis and permeability of the vascular endothelium (30). Pharmacologic inhibition of VEGFR2 activity can result in clinically relevant dose-limiting toxicities such as hypertension, thrombosis, and hemorrhage. We therefore designed BLU-667 to have enhanced activity and selectivity for RET versus VEGFR2. Whereas cabozantinib, vandetanib, and RXDX-105 displayed little to no selectivity for RET over VEGFR2, BLU-667 was 88-fold more potent against RET (Table 1). To confirm the high selectivity of BLU-667 for RET across human kinases, we screened a panel of 371 kinases for inhibition by BLU-667 at 300 nmol/L. To refine our understanding of the selectivity that BLU-667 has for RET, we determined the IC_{50} for kinases inhibited greater than 50% with 300 nmol/L BLU-667 using a highly sensitive radiometric kinase activity assay. These data showed that BLU-667 was at least 100-fold more selective for RET over 96% of kinases tested (Fig. 1C; Supplementary Table S1). Thus, BLU-667 is more potent on RET than the MKIs being studied in *RET*-driven malignancies and highly selective across human kinases.

BLU-667 Inhibits RET Signaling and Proliferation in *RET*-Driven Cancer Cell Lines

Constitutively activated RET leads to autophosphorylation of the kinase, recruitment of adapter proteins (e.g., SHC), and downstream activation of the MAPK pathway (31). To assess BLU-667 in a cellular setting, Ba/F3 cells were engineered to express a KIF5B–RET fusion and treated with BLU-667, RXDX-105, cabozantinib, or vandetanib. BLU-667 inhibited RET autophosphorylation with a cellular IC_{50} of 5 nmol/L, at least 10 times more potently than cabozantinib, vandetanib, and RXDX-105 (IC_{50} 61.9, 833, and 128.6 nmol/L, respectively; Fig. 1D). To confirm that BLU-667 suppressed RET pathway signaling, phosphorylation of RET, SHC, and ERK1/2 was measured in a panel of *RET*-driven cell lines: LC2/ad (CCDC6–RET, NSCLC), MZ-CRC-1 (RET^{M918T}, MTC), and TT (RET^{C634W}, MTC). BLU-667 inhibited phosphorylation of RET, SHC, and ERK1/2 at concentrations at or below 10 nmol/L in these cell lines (Fig. 2A–C). To confirm MAPK pathway suppression, we measured the impact of BLU-667 on expression of *DUSP6* and *SPRY4*, two genes transcriptionally regulated by ERK1/2 (32, 33). In all models tested, regardless of lineage or type of RET alteration, BLU-667 decreased the abundance of these transcripts in a dose-dependent manner but did not affect the expression of *GSK3B*, a component of the parallel PI3K–AKT pathway (Fig. 2D–F). Collectively, these data indicate that BLU-667 specifically abrogates RET signaling in *RET*-altered cancers from diverse lineages. Importantly, RET pathway inhibition with BLU-667 also more potently inhibited proliferation of *RET*-altered cell lines relative to MKIs (Supplementary Table S2).

We next assessed the activity of BLU-667 against RET V804L and V804M gatekeeper mutations which confer resistance to cabozantinib and vandetanib. In unbiased N-ethyl-N-nitrosourea (ENU) mutagenesis screens in KIF5B–RET Ba/F3 cells, we found amino acid substitution at the V804 gatekeeper position was the most common resistance mutation for all MKIs tested (cabozantinib, vandetanib, ponatinib, and regorafenib). In addition to the previously described V804L and V804M substitutions, we identified a substitution, V804E, that conferred resistance to all MKIs tested (Supplementary Table S3). Cellular screening confirmed BLU-667 suppressed proliferation of KIF5B–RET Ba/F3 cells harboring V804L, V804M, or V804E variants as potently as WT RET (Supplementary Table S2). In contrast, the activity of the MKIs was shifted 9- to 36-fold higher than that on WT RET. These data suggest the potential for BLU-667 to overcome and prevent emergence of resistance due to gatekeeper mutations.

BLU-667 Demonstrates Antitumor Activity on Diverse *RET*-Driven *In Vivo* Models

The antitumor activity of BLU-667 in multiple *RET*-driven murine tumor models was evaluated. BLU-667 showed potent

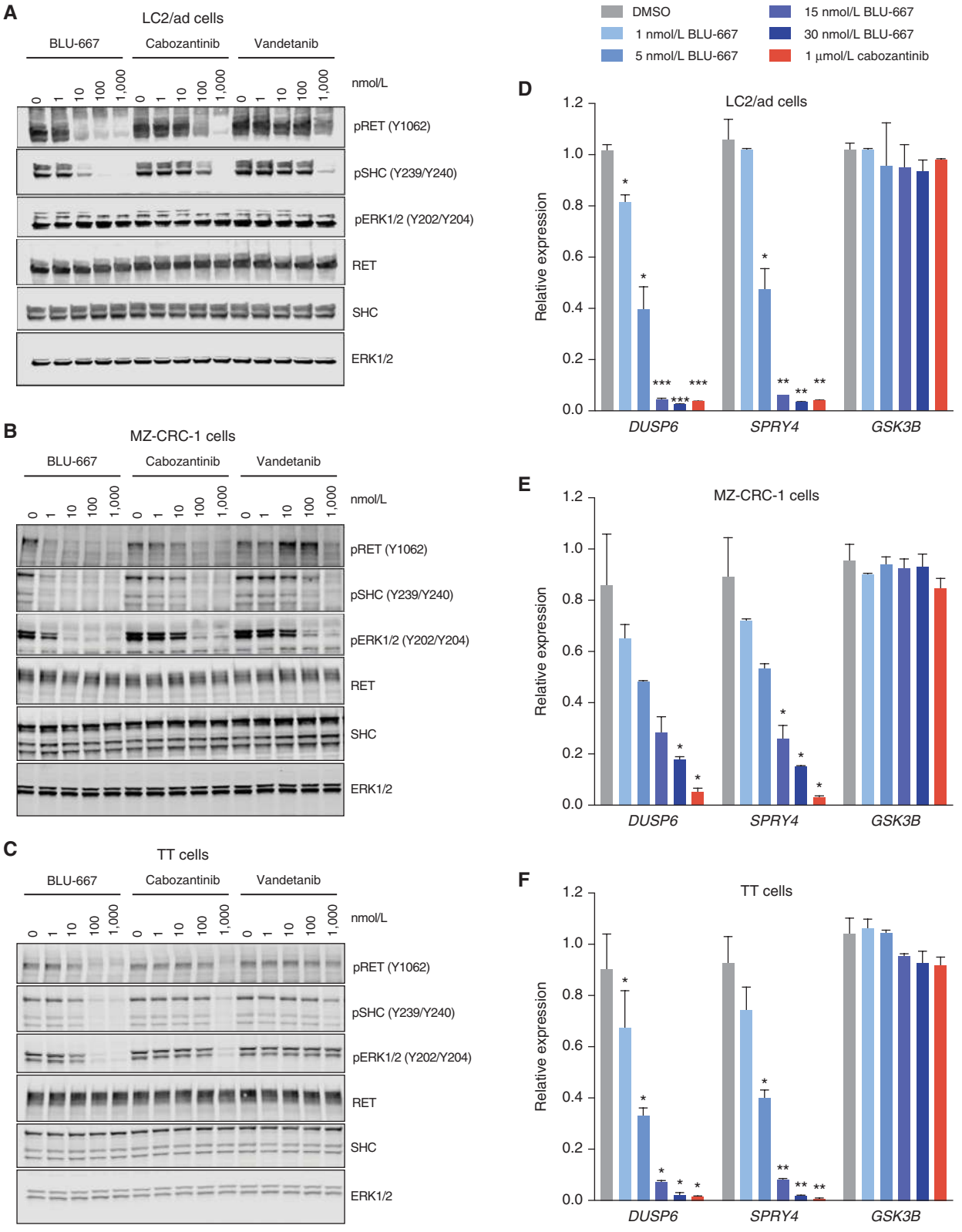

Figure 2. RET signaling pathways are inhibited by BLU-667. **A–C,** Immunoblots of whole cell lysates from (**A**) LC2/ad NSCLC cells, (**B**) MZ-CRC-1 MTC cells, or (**C**) TT MTC cells treated with BLU-667, cabozantinib, or vandetanib at indicated concentrations (nmol/L) for 90 minutes. Phospho- and total RET, SHC, and ERK1/2 were interrogated. In LC2/ad cells, pERK is represented by the top two bands of the triplet. **D–F,** Relative transcript expression of RET pathway targets *DUSP6* and *SPRY4* and AKT pathway target *GSK3B* 7 hours after treatment of (**D**) L2C/ad, (**E**) MZ-CRC-1 cells, or (**F**) TT MTC cells with BLU-667 or cabozantinib. Data are the mean + SD. *, $P < 0.05$; **, $P < 0.01$; ***, $P < 0.001$, two-sided Student *t* test. SD, standard deviation.

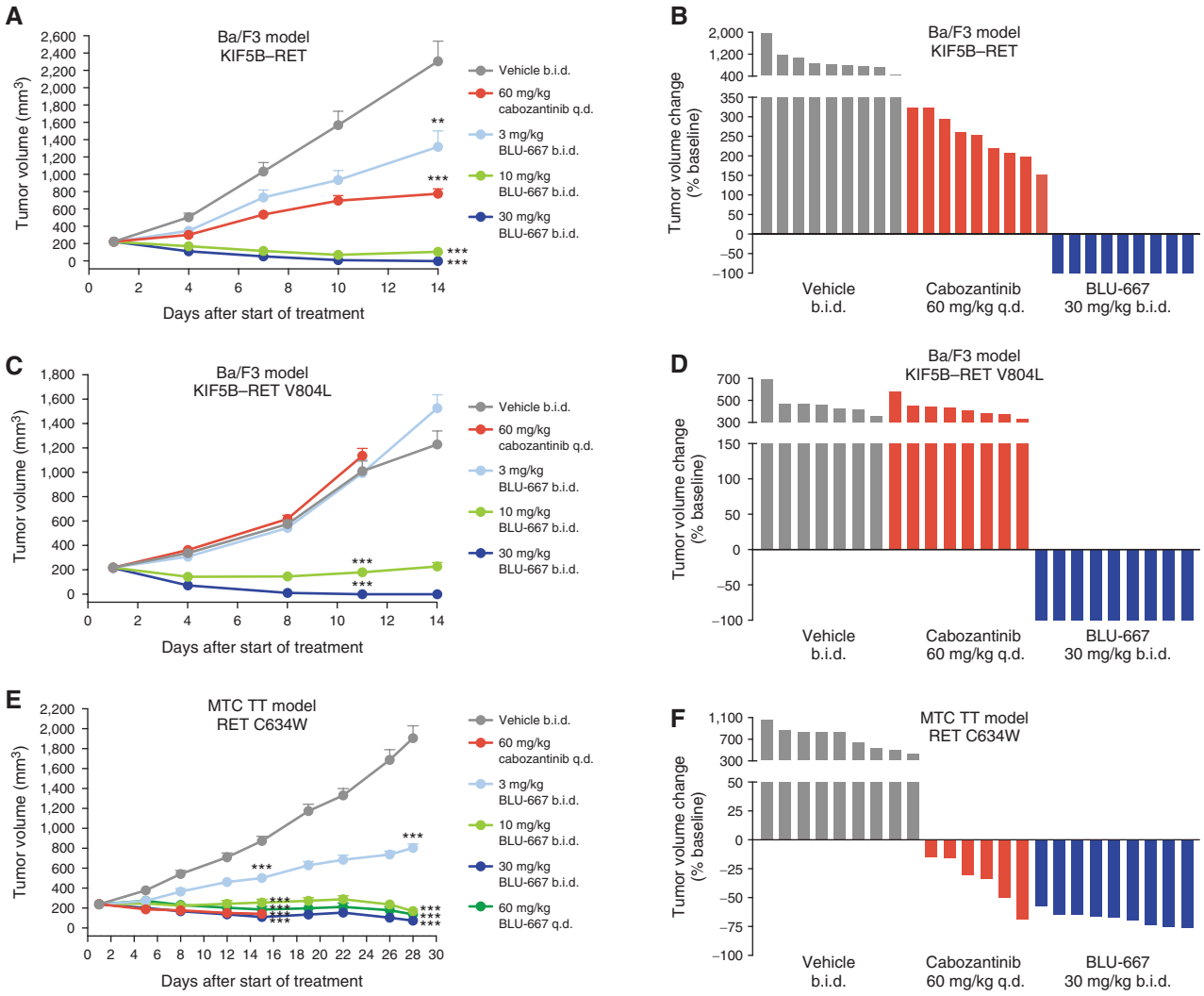

Figure 3. Antitumor activity of BLU-667 across RET-driven solid tumor models *in vivo*. Antitumor activity of BLU-667 compared with cabozantinib and waterfall plot showing the best response as a percentage change in tumor volume taken on the last day of treatment in KIF5B–RET Ba/F3 allografts (**A**, **B**), KIF5B–RET V804L Ba/F3 allografts (**C**, **D**), and RET C634W TT xenografts (**E**, **F**). Nine mice were included in each treatment group. Data are the mean + SEM. **, $P < 0.01$; ***, $P < 0.001$, one-way ANOVA with a Dunnett multiple comparisons test (RET C634W TT xenografts) or repeated measures two-way ANOVA (KIF5B–RET and KIF5B–RET V804L Ba/F3 allografts). b.i.d., twice daily; q.d., once daily.

dose-dependent activity against both KIF5B–RET Ba/F3 and KIF5B–RET^{V804L} Ba/F3 allograft tumors with doses as low as 10 mg/kg twice daily (Fig. 3A and B). In stark contrast, the V804L mutant rendered cabozantinib ineffective (Fig. 3B). Cabozantinib was tolerated poorly *in vivo*, precluding any dose increase (Supplementary Fig. S1). BLU-667 also demonstrated potent activity in a RET^{C634W} MTC xenograft (Fig. 3C) and KIF5B–RET NSCLC and CCDC6–RET colorectal cancer patient-derived xenograft (PDX) models (Fig. 4A; Supplementary Fig. S2). Thus, BLU-667 has broad *in vivo* activity against multiple oncogenic *RET* alterations, regardless of tumor type. To demonstrate that RET pathway inhibition correlated with antitumor activity *in vivo*, RET pathway inhibition was assessed in tumor lysates harvested after BLU-667 administration. BLU-667 decreased pRET and pSHC in a dose-dependent manner and maintained inhibition of both targets throughout the 12-hour dosing period at the efficacious dose of 30 mg/kg twice daily (Fig. 4B; Supplementary Fig. S3). In the KIF5B–RET NSCLC PDX, inhibition of RET phosphorylation led to a sustained decrease in expression of the MAPK target genes *DUSP6* and *SPRY4* (Fig. 4C). By contrast, 60 mg/kg once-daily cabozantinib displayed only transient suppression of *DUSP6* and *SPRY4* expression, indicating incomplete suppression of RET pathway signaling and raising the possibility that some of the antitumor activity of cabozantinib may be mediated through non-RET inhibitory mechanisms.

Increases in circulating VEGFA and decreases in soluble VEGFR2 (sVEGFR2) are two biomarkers for VEGFR2 inhibition in preclinical and clinical studies (34). To demonstrate BLU-667 specificity for RET over VEGFR2 *in vivo,* we measured plasma levels of these biomarkers in the KIF5B–RET PDX tumor-bearing mice treated with cabozantinib or BLU-667

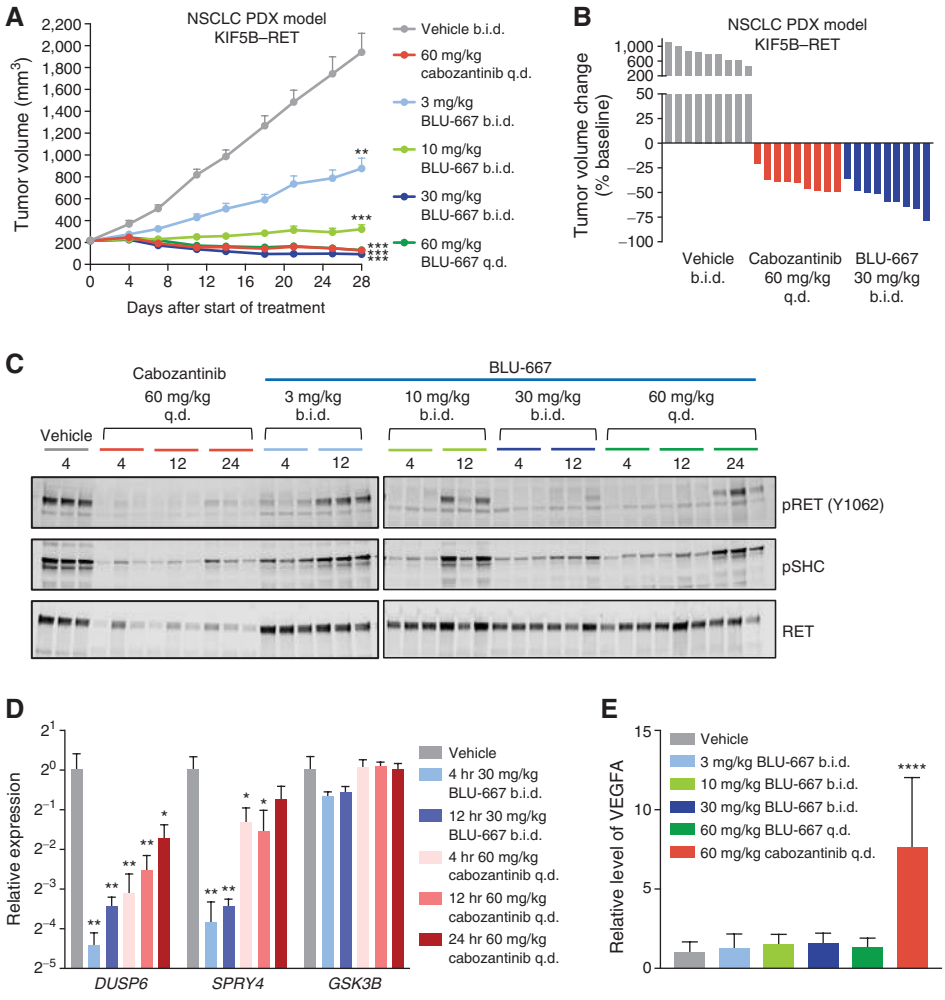

Figure 4. BLU-667 inhibits RET activity in a KIF5B–RET NSCLC PDX model while sparing VEGFR2. **A** and **B,** Antitumor activity of BLU-667 compared with cabozantinib (**A**) and waterfall plot showing the best response as a percentage change in tumor volume taken on the last day of treatment (**B**) in KIF5B–RET NSCLC PDX. Nine mice were included in each treatment group. Data are the mean + SEM. **, $P < 0.01$; ***, $P < 0.001$, one-way ANOVA with a Dunnett multiple comparisons test. **C,** Immunoblotting of tumor lysates from KIF5B–RET NSCLC PDX treated with BLU-667 and cabozantinib collected at the indicated times after administration of last dose. **D,** Relative transcript expression of *DUSP6, SPRY4,* and *GSK3B* from KIF5B–RET NSCLC PDX. Tumors collected at the indicated times (hours) after administration of last dose. Data are the mean + SD. *, $P < 0.05$; **, $P < 0.01$; ***, $P < 0.001$, two-sided Student *t* test. **E,** Circulating VEGFA from the plasma of KIF5B–RET NSCLC PDX-bearing mice treated with BLU-667 or cabozantinib. Data are the mean + SD. ***, $P < 0.001$, one-way ANOVA with a Dunnett multiple comparisons test. b.i.d., twice daily; q.d., once daily.

from the *in vivo* experiment shown in Fig. 4A. Consistent with its potent VEGFR2 biochemical activity, cabozantinib significantly increased the level of circulating VEGFA ($P < 0.001$) and decreased sVEGFR2 compared with vehicle treatment ($P = 0.01$; Fig. 4D; Supplementary Fig. S4). By contrast, BLU-667 did not significantly alter the levels of circulating VEGFA or sVEGFR2 at any dose tested. Together, these data indicate that BLU-667 potently and selectively inhibited RET without modulating VEGFR2 *in vivo*, confirming that selective RET inhibition is sufficient for antitumor activity in these preclinical tumor models.

BLU-667 Exhibits Clinical Activity in Early Studies

To investigate the clinical impact of BLU-667 on *RET*-driven malignancies, a phase I, first-in-human, dose-escalation study of BLU-667 in patients with advanced, unresectable NSCLC, thyroid cancer, or other solid tumors was initiated (NCT03037385). Both tyrosine kinase inhibitor (TKI)–naïve and TKI-refractory patients with any number of lines of therapy were eligible for enrollment in the study.

A 27-year-old patient with sporadic MTC harboring multiple *RET* mutations (L629P, D631_R635DELINSG, and V637R) was among the first patients to enroll in the first-in-human BLU-667 trial. The patient was TKI-naïve prior to the start of BLU-667 treatment, with highly invasive disease that required emergent tracheostomy and extensive surgery, including total thyroidectomy, central neck dissection, bilateral levels 1 through 4 neck dissection, total thymectomy, and median sternotomy. The postoperative course was complicated by chylothorax. Multidisciplinary medical consensus was against radiotherapy to the neck, and restaging scans showed left paratracheal disease with

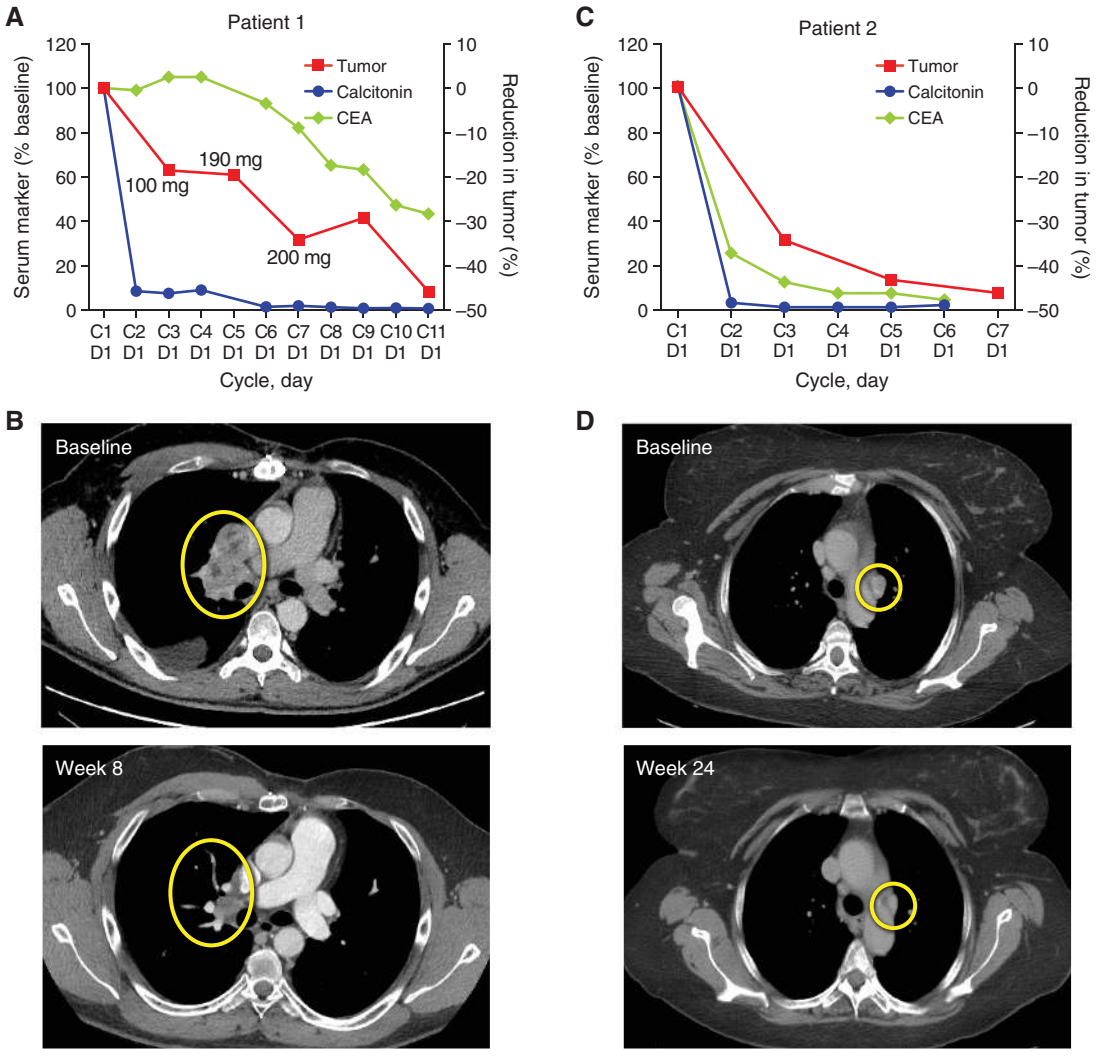

Figure 5. Rapid clinical response in RET-driven MTC tumors treated with BLU-667. **A,** Tumor size and the levels of calcitonin and CEA decreased over the course of treatment with BLU-667. Patient was treated with BLU-667 orally at 60 mg once daily initially and then received successive dose escalations up to 300 mg once daily. **B,** CT scan of tumor (circled) at baseline (top) and after 8 weeks of BLU-667 treatment (bottom) demonstrates rapid reduction in tumor volume. **C,** Tumor size and calcitonin and CEA decrease over the course of treatment with 300 mg BLU-667 once daily. **D,** CT scan of the patient's tumor (circled) at baseline (top) and after 24 weeks of BLU-667 treatment (bottom). CEA, carcinoembryonic antigen; C, cycle number; D, day.

tracheal and esophageal invasion as well as metastatic disease to the lungs and liver. The two FDA-approved multikinase drugs for MTC (vandetanib and cabozantinib) were not considered appropriate for this patient given the associated risk of VEGFR-related toxicities that can include impaired wound healing and increase the risk of fistula formation and hemorrhage (35, 36). Therefore, the patient was enrolled on the BLU-667 clinical trial and began treatment at the second dose level (60 mg, once daily). Remarkably, after 28 days of BLU-667 therapy, there was a >90% reduction in the serum tumor marker calcitonin (Fig. 5A). After 8 weeks, target lesions were reduced by 19%. After successive dose escalations of BLU-667 to 200 mg once daily, the patient achieved partial response with >30% tumor reduction per RECIST version 1.1 (Fig. 5B). This patient subsequently escalated to 300 mg once daily BLU-667 and achieved a confirmed partial response (47% maximal reduction) at 10 months. Overall, carcinoembryonic antigen (CEA) levels decreased by 57% over this period. Improved health status with BLU-667 treatment allowed for removal of the patient's tracheostomy tube and a return to baseline body weight after several kilograms of weight loss prior to treatment. BLU-667 has been well tolerated throughout 11 months of continuous treatment with the only drug-related adverse event being transient grade 1 decrease in white blood cells, which resolved without drug interruption or dose modification. This patient remains progression free and on therapy for more than 11 months.

Substantial antitumor activity was also observed in a second patient with MTC. In this case, a 56-year-old with sporadic RET^{M918T}-mutant disease, who had responded and then progressed on vandetanib, initiated therapy with BLU-667, 300 mg once daily. Early signals of clinical activity emerged

within the first few weeks of BLU-667 treatment: Serum calcitonin decreased >90% and CEA decreased by 75% after 28 days (Fig. 5C). *RET*^{M918T} circulating tumor DNA (ctDNA) decreased by 47% after 28 days and was not detectable after 56 days. Paired tumor biopsies collected pretreatment and 28 days after treatment demonstrated a 93% reduction in *DUSP6* and an 86% reduction in *SPRY4* mRNA expression, confirming RET-pathway inhibition within the tumor (Supplementary Fig. S5). Importantly, these indications of activity were confirmed by radiographic response (−35%) per RECIST 1.1 after 8 weeks (Fig. 5D). The patient tolerated BLU-667 treatment well without dose interruption; drug-related adverse events were grade 1 nausea and hyperphosphatemia. The patient continues on therapy more than 8 months with a confirmed partial response (maximum 47% reduction).

Beyond MTC, important antitumor activity was also observed in *RET*-altered NSCLC. A 37-year-old patient with metastatic NSCLC, who had progressed on cisplatin, pemetrexed, and bevacizumab, had tumor tissue test positive for a *RET* fusion via FISH analysis. The patient initiated treatment with 200 mg once daily BLU-667, and ctDNA analysis at baseline revealed a canonical *KIF5B–RET* fusion and co-occurring *TP53* mutation. Tumor reduction (−25%) was noted at first radiographic assessment after 8 weeks of treatment and correlated with a concomitant decline in *KIF5B–RET* and *TP53* ctDNA levels (Fig. 6A). The patient achieved a partial response on the second radiographic assessment after 16 weeks (Fig. 6B) and continues on treatment (more than 10 months) with a confirmed partial response. As observed in the patients with MTC described here, BLU-667 has been well tolerated, with all drug-related adverse events being grade 1 and including constipation (resolved), dry skin, rash, and leukopenia.

Consistent with the clinical activity of BLU-667 in TKI-resistant MTC, we also observed a rapid clinical response in a patient with TKI-refractory KIF5B–RET NSCLC. This

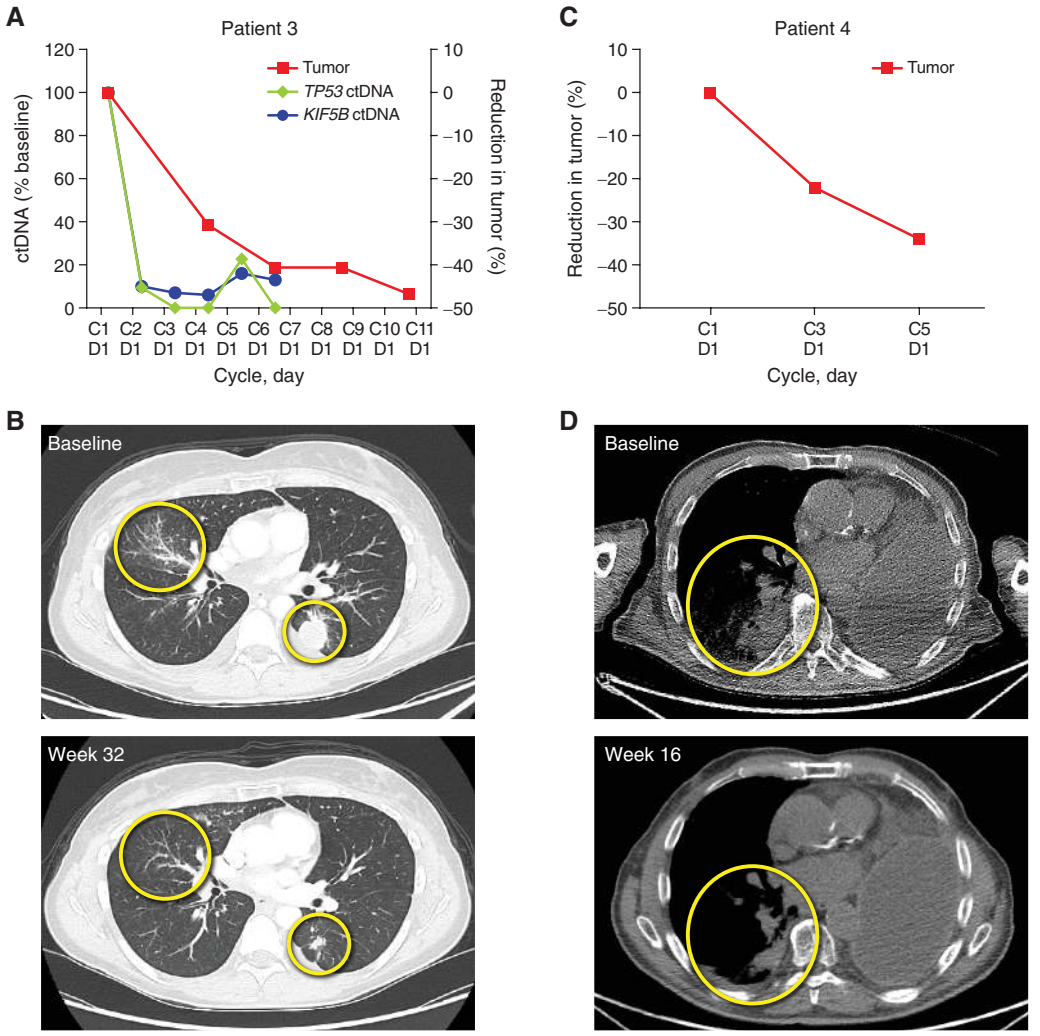

Figure 6. Partial response achieved with BLU-667 in a metastatic KIF5B–RET NSCLC tumor. **A,** Tumor and *KIF5B–RET* and *TP53* ctDNA reduction over the course of treatment with 200 mg once-daily BLU-667 demonstrates rapid response to BLU-667. **B,** CT scan illustrates tumor (circled) at baseline (top) and after 32 weeks of BLU-667 treatment (bottom). **C,** Tumor reduction over 4 cycles of treatment with 300 mg BLU-667. ctDNA not available for this patient. **D,** CT scan of the patient's tumor (circled) at baseline (top) and after 16 weeks of BLU-667 treatment (bottom). C, cycle number; D, day.

72-year-old former smoker with locally advanced NSCLC had received concurrent chemoradiation with cisplatin and pemetrexed, was then treated with carboplatin and nab-paclitaxel, and eventually progressed. Next-generation sequencing of the tumor tissue revealed a *KIF5B–RET* fusion, and the patient was enrolled on a clinical trial testing a combination regimen of vandetanib and everolimus (NCT01582191). The patient achieved a partial response, but restaging scans performed after 11 cycles showed progressive disease, which was associated with clinical symptoms of increasing dyspnea and worsening performance status. The patient was then enrolled on the phase I trial of BLU-667. After 16 weeks of BLU-667 (300 mg once daily), the patient had a partial response with 34% reduction of tumor volume (Fig. 6C and D) and improvement of dyspnea and performance status. BLU-667 has been well tolerated throughout treatment, and the patient has not experienced drug-related adverse events. This patient continues on treatment more than 18 weeks. This early clinical experience with BLU-667 demonstrates that this selective RET inhibitor can achieve response per RECIST criteria in both TKI-naïve and TKI-refractory tumors driven by *KIF5B–RET*, the most prevalent *RET* fusion found in NSCLC, and suggests the promise of this targeted therapy for this currently underserved patient population.

DISCUSSION

Targeted kinase inhibitors have produced significant improvements in the outcomes of patients across a broad range of kinase-driven cancers. This approach has been particularly successful in NSCLC, where several dysregulated tyrosine kinases such as EGFR, ALK, and ROS1 have been identified and selectively targeted, transforming a once-poor diagnosis into one with several highly effective treatment options (1, 3, 4, 37). By analogy, *RET*-rearranged NSCLC may represent a similar opportunity, as lung tumors with oncogenic RET activation typically lack other known driver mutations. Yet, despite a seemingly strong scientific rationale and precedence for precision therapy in kinase-mutated lung cancers, patients with *RET*-driven NSCLC, as well as other *RET*-driven tumors, have few good therapeutic options at present. The impact of MKIs with ancillary RET activity has been disappointing in this patient population, likely because of an inability to sufficiently inhibit oncogenic signaling driven by activating RET aberrations at maximally tolerated doses. Moreover, very much like *ALK*- and *ROS1*-rearranged NSCLC, patients with *RET*-rearranged NSCLC are characterized by a higher percentage of never-smokers than the general NSCLC population (28). As such, these tumors are likely to have a lower mutation burden and a decreased likelihood of significant benefit from immunotherapies (38–40), further underscoring the need for potent, tailored RET inhibitors.

MTC is a rare malignancy for which vandetanib and cabozantinib were approved in 2011 and 2012, respectively. However, the multikinase target profiles of these agents make their mechanisms of action unclear and their off-target safety profiles complex. In nonhereditary MTC with an estimated *RET* mutation rate of 50%, and in hereditary MTC that is almost always associated with a germline *RET* mutation, selective RET inhibition could be highly impactful and provide an additional option for patients who have progressed on, or have contraindications for, MKI therapy.

BLU-667 was designed as a potent and highly selective inhibitor of activating RET alterations found in NSCLC, thyroid cancer, and other solid tumors. BLU-667 was equally potent across various RET fusions and mutants, including CCDC6–RET, KIF5B–RET, and mutations at the gatekeeper residue: V804L, V804M, and the newly identified V804E amino acid substitution. The equipotent activity of BLU-667 across all oncogenic RET variants further differentiates it from MKIs with RET-inhibitory activity. For example, preliminary clinical trial results with RXDX-105 demonstrated no objective responses in patients with KIF5B–RET NSCLC; clinical activity was observed only among CCDC6–RET- or NCOA4–RET-driven tumors (41). This lack of response to RXDX-105 in patients with KIF5B–RET NSCLC has raised the important question of whether KIF5B–RET truly drives these tumors or whether KIF5B–RET-driven tumors have a different biology, less dependent on RET kinase activity and thus less sensitive to RET inhibition. Given the results reported here with BLU-667, this explanation of reduced RET dependence in KIF5B–RET tumors seems unlikely and is further refuted by the recent report of a KIF5B–RET NSCLC partial response per RECIST criteria observed with the RET inhibitor LOXO-292 (42). BLU-667 inhibited KIF5B–RET autophosphorylation over 20-fold more potently than RXDX-105 *in vitro* and provides a sound rationale for the preferential activity seen with BLU-667.

The combined action of MKIs on RET and VEGFR2 has been postulated by some to contribute positively to antitumor activity, especially in MTC. However, we have shown that BLU-667 was able to achieve high levels of RET inhibition and antitumor activity both preclinically and clinically without concomitant VEGFR2 inhibition, suggesting it is not required for effective treatment of RET-altered tumors and better avoided considering the associated toxicities. The closest BLU-667 kinase off-target identified in biochemical screening was JAK1, with IC_{50} shifted 20-fold relative to RET. Yet evidence of clinically significant JAK inhibition (reduced reticulocytes, red blood cells, neutrophils/monocytes) has not appeared among the four patients described above, suggesting the preferential activity of BLU-667 for RET versus JAK was preserved *in vivo*. Given this, it is unlikely that JAK inhibitory activity plays a part in the BLU-667 antitumor activity, unless only low levels of JAK inhibition are required. Future studies will illuminate the full spectrum of BLU-667 activity, but all data to date support the view that RET inhibition is sufficient for antitumor activity and that high levels of sustained target inhibition with a selective kinase inhibitor can deliver meaningful clinical responses with potentially fewer off-target side effects, making long-term drug administration more tolerable for patients.

It has been proposed that the inclusion of a pharmacodynamic assessment of molecularly targeted therapies in clinical trials can streamline the drug-development process (43, 44). Pharmacodynamic biomarkers have been successfully utilized for the clinical development of kinase inhibitors, including imatinib and gefitinib (44–46). In this study, BLU-667 dose-dependently inhibited RET and SHC activation, which

mirrored the inhibition of *DUSP6* and *SPRY4* transcription across *RET*-driven preclinical models, indicating that these transcripts can serve as biomarkers for RET inhibitory activity. The translational capability of these markers was established in this study in which MTC tumor shrinkage induced by BLU-667 treatment was associated with efficient inhibition of *DUSP6* and *SPRY4* expression within the tumor tissue. To our knowledge, this represents the first confirmation of RET target engagement by a small-molecule inhibitor, multitargeted or selective, within the clinical setting and may be used in this and future studies to more precisely define the optimal dose and schedule required for effective RET inhibition.

The specificity and potency of BLU-667 for RET, its preliminary antitumor activity in patients with *RET*-altered MTC or NSCLC, and its seemingly favorable clinical safety profile in these early studies suggest that BLU-667 has potential to improve outcomes in patients with *RET*-driven cancers while limiting off-target adverse effects. Importantly, selective RET inhibition by BLU-667 was sufficient for antitumor activity, in patients with KIF5B–RET NSCLC that were TKI naïve or TKI refractory and in a patient with vandetanib-resistant MTC. By offering a highly selective medicine specifically tailored for the oncogenic driver, we hope BLU-667 will enable patients with *RET*-driven tumors to benefit from the recent advances in genomic profiling that have revolutionized treatment options for patients with kinase-driven diseases.

METHODS

BLU-667 Synthesis

The synthesis of BLU-667 is described in WO 2017/079140; example 5, compound 130 (47). Details can be found at https://patentscope.wipo.int/search/en/detail.jsf?docId=WO2017079140.

In Vitro *Biochemical Activity Assay*

Recombinant RET enzyme and enzyme variants (V804L, V804M, M918T, and CCDC6-RET) were purchased from ProQinase GmbH, and recombinant VEGFR2 enzyme was purchased from Carna Bio USA, all containing N-terminal Glutathione S-transferase tags. Cabozantinib, vandetanib, and RXDX-105 were purchased from Selleck Chemicals. Kinase/peptide substrate pairs, serially diluted compounds, and cofactors required were prepared in a reaction buffer at their respective Michaelis constant ($^{APP}K_M$) for ATP and incubated for 120 minutes. The reactions were stopped by the addition of an EDTA-containing buffer and proportional enzymatic activities were measured using the Perkin Elmer electrophoretic mobility shift platform (EZReader, Perkin Elmer). Potency was calculated from EZReader data with 1% DMSO and 10 μmol/L regorafenib as 0 and 100% inhibition controls. Half maximal inhibitory concentration (IC_{50}) was calculated using a 3-paramenter fit in Core LIMS (top constraint = 100).

Human Kinase Selectivity

BLU-667 was screened at 300 nmol/L for inhibitory activity across a panel of 371 kinases (Reaction Biology Corporation). The 23 kinases inhibited >50% at 300 nmol/L were selected for full 10 point concentration–response curves with BLU-667 (1 μmol/L maximum concentration) at 200 μmol/L ATP to generate biochemical IC_{50} (Reaction Biology Corp) using ^{33}P-ATP (10 mCi/mL) to initiate the reaction, followed by the detection of kinase activity by a filter-binding method.

Cell Culture

The TT MTC cell line was purchased from the ATCC (2014) and grown in 20% FBS Ultraculture with GlutaMAX (ThermoFisher Scientific). LC2/ad was obtained from Riken (2014) and grown in 1:1 Ham's F12:RPMI medium supplemented with 15% FBS, 1 × penicillin–streptomycin, and 25 mmol/L 4-(2-hydroxyethyl)-1-piperazineethanesulfonic acid (HEPES). MZ-CRC-1 and TPC-1 cell lines were obtained in 2014 from the University of Colorado Denver. MZ-CRC-1 cells were grown in DMEM with 10% FBS; TPC-1 cells were grown in RPMI medium with 10% FBS. Parental Ba/F3 cells were purchased from Leibniz Institute DSMZ German Collection of Microorganisms and Cell Culture (2013) and grown in RPMI medium with 10% FBS, 1 × penicillin–streptomycin, and 5 ng/mL murine interleukin-3 (mIL3). Ba/F3 KIF5B–RET cell lines were grown in RPMI medium with 10% FBS, 1 × penicillin–streptomycin, and 1 ng/mL doxycycline. Cell lines were authenticated by periodic short tandem repeat (STR) profiling (PowerPlex 16HS by Promega, testing performed at Genetica) and confirmed to be *Mycoplasma* free (PCR-based detection by DDC Medical and Genetica). TT cells were last authenticated by STR in May 2015, LC2/ad in August 2016, MZ-CRC-1 in March 2017. Ba/F3 cells were not authenticated. Cell lines were last tested for *Mycoplasma* in August 2016 (LC2/ad, TT) and August 2017 (MZ-CRC-1, Ba/F3). All cell lines were thawed and passaged at least 3 times before initiating experiments. Cells were discarded after 18 passages.

Generation of KIF5B–RET Ba/F3 Cells

The DNA encoding the amino acid sequence of human *KIF5B–RET* variant 1 was placed in a lentivirus vector under a doxycycline-inducible promoter to maximize expression with a carboxyl-terminal FLAG epitope to facilitate immunodetection of the fusion by anti-FLAG antibodies. Lentiviral-mediated gene transduction was used to express *KIF5B–RET* in Ba/F3 cells; KIF5B–RET-dependent cells were selected by IL3 withdrawal and confirmed to express the KIF5B–RET fusion protein by immunoblot analysis.

Proliferation Assays

KIF5B–RET Ba/F3 cells were exposed to compound concentrations ranging from 25 μmol/L to 95.4 pmol/L for 48 hours, and proliferation was assessed with Cell Titer Glo (Promega). TT, MZ-CRC-1, TPC-1, or LC2/ad cells were exposed to compound for 4 days and proliferation was measured by BrdUrd incorporation (Abcam). The luminescence of the samples was measured on an EnVision reader (PerkinElmer Inc.) with a 1-second integration time. IC_{50} for proliferation curves were calculated using a 4-parameter logistic nonlinear regression model in Core LIMS (Core Informatics LLC).

ENU Mutagenesis Assays

To generate Ba/F3 cells carrying V804 substitutions, WT KIF5B–RET Ba/F3 cells were mutagenized overnight with ENU and plated in 96-well plates for a period of 2 weeks in the presence of 6 concentrations of MKIs (ponatinib, regorafenib, cabozantinib, or vandetanib). The concentrations chosen ranged from 2× to 64× the proliferation IC_{50} for each compound: 125 nmol/L to 4 μmol/L cabozantinib, 20 to 640 nmol/L ponatinib, and 250 nmol/L to 8 μmol/L vandetanib. Genomic DNA was isolated from resistant clones, and Sanger sequencing was used to identify those that harbored substitutions.

Immunoblots

Cells were treated with the indicated compound concentrations for 90 minutes. For all cell lines except LC2/ad, cell pellets were lysed in Phospho-Safe lysis buffer (EMD Millipore). To lyse the LC2/ad cells, 1 × NuPAGE lithium dodecyl sulfate (LDS) sample buffer (Thermo Fisher Scientific) with 5% 2-mercaptoethanol preheated to 95°C was

added to each well. Total cell lysates were resolved by SDS-PAGE and transferred onto nitrocellulose membranes (Bio-Rad). Primary antibodies included phospho-RET (Y1062, sc-20252-R; Santa Cruz Biotechnology), total RET (#3223; Cell Signaling Technology), phospho-SHC (Y239/Y240, #2434; Cell Signaling Technology), phospho-ERK1/2 (T202/Y204, #4370; Cell Signaling Technology), total ERK1/2 (#9107; Cell Signaling Technology), total SHC antibody (06-203; EMD Millipore), and total Beta-Actin (ab3280; Abcam). Secondary antibodies (IRDye 800–conjugated rabbit IgG and IRDye 700–conjugated mouse IgG) were from Rockland Immunochemicals Inc. Immunoblots were imaged using the Odyssey fluorescent imaging system (LI-COR Biosciences).

AlphaLISA Phospho-RET Assay

Cell lines were exposed to BLU-667 or reference compound for 90 minutes and lysed with AlphaLISA Lysis Buffer (Perkin Elmer) supplemented with protease/phosphatase inhibitors. Autophosphorylated RET was detected with antibody against phospho-RET Y1062 (sc-20252-R, Santa Cruz Biotechnology). Anti-FLAG donor beads (Perkin Elmer) or anti-Rabbit acceptor beads (Perkin Elmer) were added to cell lysates and agitated for 1 hour each. An EnVision Multilabel Reader (PerkinElmer) was used to detect the AlphaLISA signal. IC_{50} was calculated using a 4-parameter logistic nonlinear regression model in Core LIMS.

DUSP6 and SPRY4 Expression Analysis

Cells were treated with the indicated compounds for 7 hours before lysis with Buffer RLT (QIAGEN) containing 1% β-mercaptoethanol. Total RNA was isolated using the RNeasy Plus Mini Kit (QIAGEN) according to the manufacturer's instructions. First-strand cDNA was synthesized using the SuperScript VILO Master Mix (Thermo Fisher Scientific) according to the manufacturer's instructions. Real-time qPCR was run on the ViiA 7 Real Time PCR System (Thermo Fisher Scientific). For qRT-PCR, the expression of the reference gene glucuronidase beta (*GUSB*) was used to normalize expression of the target genes *DUSP6, SPRY4*, and glycogen synthase kinase 3 beta (*GSK3B*). Replicate qRT-PCR reactions were analyzed for each sample, and QuantStudio Real-Time PCR software (Life Technologies) normalized the average expression of *DUSP6, SPRY4*, or *GSK3B* to the average expression of the reference gene *GUSB* in each sample.

Animal Studies

All procedures relating to animal handling, care, and treatment were performed according to the guidelines approved by the Institutional Animal Care and Use Committee of the contract research organizations performing the study, following the guidance of the Association for Assessment and Accreditation of Laboratory Animal Care. Allograft and xenograft models using cell lines were performed at Shanghai ChemPartner, and BALB/c nude mice were inoculated subcutaneously into the right flank with 1×10^7 KIF5B–RET Ba/F3 cells, 5×10^6 KIF5B–RET V804L Ba/F3 cells, or 1×10^7 TT cells. Mice were divided into groups of 9, and treatments began when tumors were between 217 and 238 mm^3. For PDX tumor models, CTG-0838 NSCLC PDX (Champions Oncology) or CR2518 colorectal cancer PDX (CrownBio) tumor fragments were implanted subcutaneously in the left flank of nu/nu nude mice or right flank of BALB/c nude mice, respectively. Mice were divided into groups of 9, and treatments began when tumors reached 215 or 151 mm^3 for NSCLC and colorectal cancer PDX tumors, respectively. For all experiments, mice were dosed twice daily with vehicle, 3, 10, or 30 mg/kg BLU-667 or once daily with 60 mg/kg BLU-667 or 60 mg/kg cabozantinib. For measurement of RET, ERK1/2, and SHC phosphorylation and *DUSP6/SPRY4* expression in NSCLC PDX tumors, tumor lysates were collected 4, 12, and 24 hours following the last doses of 60 mg/kg cabozantinib or 60 mg/kg BLU-667, and 4 and 12 hours following the last doses of 3, 10, or 30 mg/kg BLU-667. Phosphorylation of RET signaling components was measured using immunoblotting. Transcription of *DUSP6/SPRY4* was measured using qPCR as above. For assessment of VEGFR2 inhibition, Quantikine ELISA kits (R&D Systems) were used for the quantitative determination of mouse soluble VEGFR2 and VEGFA from mouse plasma. Protocols were performed according to the manufacturer's instructions.

BLU-667 Phase I Study

A phase I, first-in-human study (NCT03037385) to define the maximum tolerated dose, safety profile, pharmacokinetics, and preliminary antitumor activity of BLU-667 in advanced, *RET*-altered NSCLC, MTC, and other solid tumors was initiated in March 2017. The study was conducted in accordance with ethical principles founded in the Declaration of Helsinki and was reviewed and approved by the institutional review board of each clinical site. Prior to study entry, written informed consent was obtained from all patients for treatment with BLU-667 and collection of blood and tumor samples for exploratory biomarker analyses to characterize potential predictive biomarkers of safety and efficacy. Adult patients (≥18 years of age) must have had advanced, unresectable solid tumors, with an Eastern Cooperative Oncology Group performance status of 0 to 2, and adequate bone marrow, hepatic, renal, and cardiac function. BLU-667 was administered orally, once daily, on a 4-week cycle using a Bayesian Optimal Interval Design. At dose levels ≥120 mg, documented *RET* alteration was additionally required for study entry. Adverse events were graded per Common Terminology Criteria for Adverse Events (CTCAE). Radiographic response by computed tomography was evaluated RECIST version 1.1. Levels of ctDNA in plasma were assessed using the PlasmaSELECT-R64 NGS panel (Personal Genome Diagnostics). Serum calcitonin levels in patietnts with MTC were measured by ELISA (Medpace). Tumor *DUSP6/SPRY4* levels were analyzed by qRT-PCR (Molecular MD). Presented data are preliminary and represent a data cutoff of March 23, 2018.

Statistical Analyses

Statistical comparisons of tumor volumes as well as VEGFA and sVEGFR2 plasma levels were conducted using a one-way ANOVA followed by a Games–Howell or Dunnett multiple comparisons test comparing treatment groups with the control group or a repeated measures two-way ANOVA. Statistical comparisons of the *DUSP6* and *SPRY4* levels were conducted using a two-sided Student *t* test. For all comparisons, $P < 0.05$ was considered statistically significant.

Disclosure of Potential Conflicts of Interest

V. Subbiah reports receiving commercial research grants from Blueprint Medicines, Fujifilm, BERG, PharmaMar, D3, Pfizer, Loxo Oncology, MultiVir, Amgen, AbbVie, Roche/Genentech, Novartis, Incyte, Idera Pharmaceuticals, Bayer, GlaxoSmithKline, NanoCarrier, Vegenics, and Northwest Biotherapeutics. J.F. Gainor is a consultant/advisory board member for Bristol-Myers Squibb, Takeda, Novartis, Amgen, Pfizer, Genentech/Roche, Loxo, Merck, Incyte, Array Biopharma, and Theravance. R. Rahal has ownership interest in Blueprint Medicines. J.D. Brubaker has ownership interest in Blueprint Medicines. J.L. Kim has ownership interest in Blueprint Medicines. W. Hu has ownership interest in Blueprint Medicines. Q. Cao has ownership interest in Blueprint Medicines. M.P. Sheets has ownership interest in Blueprint Medicines. D. Wilson has ownership interest in Blueprint Medicines. K.J. Wilson has ownership interest in Blueprint Medicines. L. DiPietro has ownership interest in Bluerprint Medicines. M.I. Hu reports receiving commercial research support from Sanofi Genzyme. L. Wirth is a consultant/advisory board member for Eisai, Blueprint, and Loxo. M.S. Brose is a consultant/advisory board member for Blueprint Medicines. M. Taylor has received honoraria

from the speakers bureaus of Bristol-Myers Squibb and Eisai Inc. and is a consultant/advisory board member for Loxo Oncology, Novartis, Blueprint Medicines, and Roche/Genentech. E. Garralda is a consultant/advisory board member for Roche and NeoMed Therapeutics. B. Wolf has ownership interest (including patents) in Blueprint Medicines. C. Lengauer has ownership interest in Blueprint Medicines. T. Guzi has ownership interest in Blueprint Medicines. E.K. Evans has ownership interest in Blueprint Medicines. No potential conflicts of interest were disclosed by the other authors.

Authors' Contributions

Conception and design: V. Subbiah, R. Rahal, J.D. Brubaker, W. Hu, L. DiPietro, P. Fleming, M. Palmer, L. Wirth, M.S. Brose, S. Miller, B. Wolf, C. Lengauer, T. Guzi, E.K. Evans

Development of methodology: V. Subbiah, R. Rahal, J.D. Brubaker, W. Hu, Q. Cao, K.J. Wilson, L. DiPietro, M. Palmer, L. Wirth, M.S. Brose, B. Wolf, T. Guzi

Acquisition of data (provided animals, acquired and managed patients, provided facilities, etc.): V. Subbiah, J.F. Gainor, M. Maynard, W. Hu, Q. Cao, M. Palmer, M.I. Hu, L. Wirth, M.S. Brose, S.-H. Ignatius Ou, M. Taylor, E. Garralda, B. Wolf, E.K. Evans

Analysis and interpretation of data (e.g., statistical analysis, biostatistics, computational analysis): V. Subbiah, J.F. Gainor, R. Rahal, J.D. Brubaker, J.L. Kim, M. Maynard, W. Hu, Q. Cao, P. Fleming, M. Palmer, M.I. Hu, L. Wirth, M.S. Brose, S.-H. Ignatius Ou, E. Garralda, B. Wolf, C. Lengauer, T. Guzi, E.K. Evans

Writing, review, and/or revision of the manuscript: V. Subbiah, J.F. Gainor, R. Rahal, J.D. Brubaker, J.L. Kim, M. Maynard, Q. Cao, M. Palmer, M.I. Hu, L. Wirth, M.S. Brose, S.-H. Ignatius Ou, M. Taylor, E. Garralda, S. Miller, B. Wolf, C. Lengauer, T. Guzi, E.K. Evans

Administrative, technical, or material support (i.e., reporting or organizing data, constructing databases): V. Subbiah, R. Rahal, J.D. Brubaker, M. Maynard, M.P. Sheets, T. Guzi, E.K. Evans

Study supervision: V. Subbiah, R. Rahal, M.I. Hu, B. Wolf, C. Lengauer, E.K. Evans

Other (compound design and synthesis): D. Wilson, L. DiPietro

Acknowledgments

We thank our colleagues at Blueprint Medicines for the thoughtful discussions and constructive feedback throughout the BLU-667 program and for the critical review of the manuscript. We also thank the scientists at Shanghai ChemPartner, CrownBio, and Champions Oncology for their excellent *in vivo* study support and execution, and Allison Cherry, PhD, of Team9 Science for medical writing support. Finally, we thank the patients and their families and the doctors and nurses for their participation in the ongoing phase I clinical trial with BLU-667. This work was funded by Blueprint Medicines.

Received March 30, 2018; revised April 9, 2018; accepted April 11, 2018; published first April 15, 2018.

REFERENCES

1. Ku GY, Haaland BA, de Lima Lopes G Jr. Gefitinib vs. chemotherapy as first-line therapy in advanced non-small cell lung cancer: meta-analysis of phase III trials. Lung Cancer 2011;74:469–73.
2. O'Brien SG, Guilhot F, Larson RA, Gathmann I, Baccarani M, Cervantes F, et al. Imatinib compared with interferon and low-dose cytarabine for newly diagnosed chronic-phase chronic myeloid leukemia. N Engl J Med 2003;348:994–1004.
3. Shaw AT, Kim DW, Nakagawa K, Seto T, Crino L, Ahn MJ, et al. Crizotinib versus chemotherapy in advanced ALK-positive lung cancer. N Engl J Med 2013;368:2385–94.
4. Zhou C, Wu YL, Chen G, Feng J, Liu XQ, Wang C, et al. Erlotinib versus chemotherapy as first-line treatment for patients with advanced EGFR mutation-positive non-small-cell lung cancer (OPTIMAL, CTONG-0802): a multicentre, open-label, randomised, phase 3 study. Lancet Oncol 2011;12:735–42.
5. Soria JC, Ohe Y, Vansteenkiste J, Reungwetwattana T, Chewaskulyong B, Lee KH, et al. Osimertinib in untreated EGFR-mutated advanced non-small-cell lung cancer. N Engl J Med 2018;378:113–25.
6. Lin JJ, Shaw AT. Resisting resistance: targeted therapies in lung cancer. Trends Cancer 2016;2:350–64.
7. Gainor JF, Shaw AT. Emerging paradigms in the development of resistance to tyrosine kinase inhibitors in lung cancer. J Clin Oncol 2013;31:3987–96.
8. Peters S, Camidge DR, Shaw AT, Gadgeel S, Ahn JS, Kim DW, et al. Alectinib versus crizotinib in untreated ALK-positive non-small-cell lung cancer. N Engl J Med 2017;377:829–38.
9. Jabbour E, Kantarjian H, Cortes J. Use of second- and third-generation tyrosine kinase inhibitors in the treatment of chronic myeloid leukemia: an evolving treatment paradigm. Clin Lymphoma Myeloma Leuk 2015;15:323–34.
10. Gainor JF, Shaw AT. The new kid on the block: RET in lung cancer. Cancer Discov 2013;3:604–6.
11. Ju YS, Lee WC, Shin JY, Lee S, Bleazard T, Won JK, et al. A transforming KIF5B and RET gene fusion in lung adenocarcinoma revealed from whole-genome and transcriptome sequencing. Genome Res 2012;22:436–45.
12. Kohno T, Ichikawa H, Totoki Y, Yasuda K, Hiramoto M, Nammo T, et al. KIF5B–RET fusions in lung adenocarcinoma. Nat Med 2012;18:375–7.
13. Stransky N, Cerami E, Schalm S, Kim JL, Lengauer C. The landscape of kinase fusions in cancer. Nat Commun 2014;5:4846–56.
14. Ballerini P, Struski S, Cresson C, Prade N, Toujani S, Deswarte C, et al. RET fusion genes are associated with chronic myelomonocytic leukemia and enhance monocytic differentiation. Leukemia 2012;26:2384–9.
15. Le Rolle AF, Klempner SJ, Garrett CR, Seery T, Sanford EM, Balasubramanian S, et al. Identification and characterization of RET fusions in advanced colorectal cancer. Oncotarget 2015;6:28929–37.
16. Skalova A, Stenman G, Simpson RHW, Hellquist H, Slouka D, Svoboda T, et al. The role of molecular testing in the differential diagnosis of salivary gland carcinomas. Am J Surg Pathol 2018;42:e11–e27.
17. Romei C, Ciampi R, Elisei R. A comprehensive overview of the role of the RET proto-oncogene in thyroid carcinoma. Nat Rev Endocrinol 2016;12:192–202.
18. Mulligan LM. RET revisited: expanding the oncogenic portfolio. Nat Rev Cancer 2014;14:173–86.
19. Tong Q, Xing S, Jhiang SM. Leucine zipper-mediated dimerization is essential for the PTC1 oncogenic activity. J Biol Chem 1997;272:9043–7.
20. Takahashi M, Ritz J, Cooper GM. Activation of a novel human transforming gene, ret, by DNA rearrangement. Cell 1985;42:581–8.
21. Yakes FM, Chen J, Tan J, Yamaguchi K, Shi Y, Yu P, et al. Cabozantinib (XL184), a novel MET and VEGFR2 inhibitor, simultaneously suppresses metastasis, angiogenesis, and tumor growth. Mol Cancer Ther 2011;10:2298–308.
22. Carlomagno F, Vitagliano D, Guida T, Ciardiello F, Tortora G, Vecchio G, et al. ZD6474, an orally available inhibitor of KDR tyrosine kinase activity, efficiently blocks oncogenic RET kinases. Cancer Res 2002;62:7284–90.
23. Drilon A, Rekhtman N, Arcila M, Wang L, Ni A, Albano M, et al. Cabozantinib in patients with advanced RET-rearranged non-small-cell lung cancer: an open-label, single-centre, phase 2, single-arm trial. Lancet Oncol 2016;17:1653–60.
24. Lee SH, Lee JK, Ahn MJ, Kim DW, Sun JM, Keam B, et al. Vandetanib in pretreated patients with advanced non-small cell lung cancer-harboring RET rearrangement: a phase II clinical trial. Ann Oncol 2017;28:292–7.
25. Yoh K, Seto T, Satouchi M, Nishio M, Yamamoto N, Murakami H, et al. Vandetanib in patients with previously treated RET-rearranged advanced non-small-cell lung cancer (LURET): an open-label, multicentre phase 2 trial. Lancet Respir Med 2017;5:42–50.
26. Shaw AT, Kim DW, Mehra R, Tan DS, Felip E, Chow LQ, et al. Ceritinib in ALK-rearranged non-small-cell lung cancer. N Engl J Med 2014;370:1189–97.

27. Drilon A, Hu ZI, Lai GGY, Tan DSW. Targeting RET-driven cancers: lessons from evolving preclinical and clinical landscapes. Nat Rev Clin Oncol 2018;15:151–67.
28. Wang R, Hu H, Pan Y, Li Y, Ye T, Li C, et al. RET fusions define a unique molecular and clinicopathologic subtype of non-small-cell lung cancer. J Clin Oncol 2012;30:4352–9.
29. Carlomagno F, Guida T, Anaganti S, Vecchio G, Fusco A, Ryan AJ, et al. Disease associated mutations at valine 804 in the RET receptor tyrosine kinase confer resistance to selective kinase inhibitors. Oncogene 2004;23:6056–63.
30. Karkkainen MJ, Petrova TV. Vascular endothelial growth factor receptors in the regulation of angiogenesis and lymphangiogenesis. Oncogene 2000;19:5598–605.
31. Takahashi M. The GDNF/RET signaling pathway and human diseases. Cytokine Growth Factor Rev 2001;12:361–73.
32. Buffet C, Hecale-Perlemoine K, Bricaire L, Dumont F, Baudry C, Tissier F, et al. DUSP5 and DUSP6, two ERK specific phosphatases, are markers of a higher MAPK signaling activation in BRAF mutated thyroid cancers. PLoS One 2017;12:e0184861.
33. Ozaki K, Kadomoto R, Asato K, Tanimura S, Itoh N, Kohno M. ERK pathway positively regulates the expression of Sprouty genes. Biochem Biophys Res Commun 2001;285:1084–8.
34. Ebos JM, Lee CR, Christensen JG, Mutsaers AJ, Kerbel RS. Multiple circulating proangiogenic factors induced by sunitinib malate are tumor-independent and correlate with antitumor efficacy. Proc Natl Acad Sci U S A 2007;104:17069–74.
35. CAPRELSA (vandetanib) [package insert]. Cambridge, MA: Sanofi Genzyme; 2016.
36. COMETRIQ (cabozantinib) [package insert]. South San Francisco, CA: Exelixix, Inc.; 2018.
37. Shaw AT, Ou SH, Bang YJ, Camidge DR, Solomon BJ, Salgia R, et al. Crizotinib in ROS1-rearranged non-small-cell lung cancer. N Engl J Med 2014;371:1963–71.
38. Borghaei H, Paz-Ares L, Horn L, Spigel DR, Steins M, Ready NE, et al. Nivolumab versus docetaxel in advanced nonsquamous non-small-cell lung cancer. N Engl J Med 2015;373:1627–39.
39. Lee CK, Man J, Lord S, Links M, Gebski V, Mok T, et al. Checkpoint inhibitors in metastatic EGFR-mutated non-small cell lung cancer-a meta-analysis. J Thorac Oncol 2017;12:403–7.
40. Sarfaty M, Moore A, Neiman V, Dudnik E, Ilouze M, Gottfried M, et al. RET fusion lung carcinoma: response to therapy and clinical features in a case series of 14 patients. Clin Lung Cancer 2017;18:e223–e32.
41. Drilon AE, Liu S, Doebele R, Rodriguez C, Fakih M, Reckamp KL, et al. LBA19 A Phase 1b study of RXDX-105, a VEGFR-sparing potent RET inhibitor, in RETi-naive patients with RET fusion-positive NSCLC. Ann Oncol 2017;28:v605–v49.
42. Velcheti V, Bauer T, Subbiah V, Cabanillas M, Lakhani N, Wirth L, et al. OA 12.07 LOXO-292, a potent, highly selective RET inhibitor, in MKI-resistant RET fusion-positive lung cancer patients with and without brain metastases. J Thorac Oncol 2017;12:S1778.
43. Tan DS, Thomas GV, Garrett MD, Banerji U, de Bono JS, Kaye SB, et al. Biomarker-driven early clinical trials in oncology: a paradigm shift in drug development. Cancer J 2009;15:406–20.
44. Sarker D, Workman P. Pharmacodynamic biomarkers for molecular cancer therapeutics. Adv Cancer Res 2007;96:213–68.
45. Baselga J, Albanell J, Ruiz A, Lluch A, Gascon P, Guillem V, et al. Phase II and tumor pharmacodynamic study of gefitinib in patients with advanced breast cancer. J Clin Oncol 2005;23:5323–33.
46. Druker BJ, Talpaz M, Resta DJ, Peng B, Buchdunger E, Ford JM, et al. Efficacy and safety of a specific inhibitor of the BCR-ABL tyrosine kinase in chronic myeloid leukemia. N Engl J Med 2001;344:1031–7.
47. Brubaker JD, Kim JL, Wilson KJ, Wilson D, Dipietro LV, inventors; Blueprint Medicines Corporation, assignee. Inhibitors of RET. International application PCT/US2016/059879. Nov 5 2017.